IEEE Access
Multidisciplinary : Rapid Review : Open Access Journal

Received May 12, 2020, accepted May 20, 2020, date of publication May 25, 2020, date of current version June 5, 2020.

Digital Object Identifier 10.1109/ACCESS.2020.2997093

Robust Control for Nonlinear Delta Parallel Robot With Uncertainty: An Online Estimation Approach

RUIYING ZHAO[1], (Member, IEEE), LINLIN WU[1], (Student Member, IEEE), AND YE-HWA CHEN[2]

[1]National Engineering Laboratory for Highway Maintenance Equipment, Chang'an University, Xi'an 710065, China
[2]The George W. Woodruff School of Mechanical Engineering, Georgia Institute of Technology, Atlanta, GA 30332, USA

Corresponding author: Ye-Hwa Chen (yehwa.chen@me.gatech.edu)

This work was supported in part by the National Natural Science Foundation of China under Grant 51605038, in part by the Shaanxi Province Natural Science Foundation under Grant 2020JM-240, and in part by the Fundamental Research Funds for Chinese Central Universities under Grant 300102258305.

ABSTRACT A series of fractional robust trajectory tracking controls are proposed for the Delta parallel robot with uncertainty. For the high speed and heavy load, the Delta parallel robot could not ignore the influences of the high nonlinearity (by the dynamics of the multiple closed-loops mechanism and the nonlinear joints friction) and the various kinds of uncertainties (i.e., the unknown dynamic parameters and external disturbances caused by the residual vibration). By formulating the motion equation of the Delta parallel robot, the nonlinearity is settled by a norm model based control design. The uncertainty considered in the paper is time-varying but unknown. An online estimation with an exponential type leakage term and dead-zone is construct to investigate the realtime information of the uncertainty. In virtue of the estimated information, two fractional robust trajectory tracking controls with the joints friction compensation are designed. Under the proposed controls, the system performance of the Delta parallel robot can be deterministically guaranteed (which includes uniform boundedness and uniform ultimate boundedness).

INDEX TERMS Delta parallel robot, fractional robust control, trajectory tracking, online estimation.

I. INTRODUCTION

Parallel robot is a kind of multiple closed-loop mechanism and widely used in the industrial areas by virtue of the high rigidity, high accuracy and outstanding weight/load ratio [1], [2]. The Delta parallel robot with three lightweight parallelograms, one of the most popular parallel robot, inherits all the virtues of the traditional parallel robots and possesses some distinct features such as, the closed form kinematics (both forward and inverse), the decoupled translational positions and rotational orientations of the moving platform (which improves the motion accuracy). Motivated by the above features, the Delta parallel robot has been applied in many sophisticated fields, e.g., microelectronics [3], [4], medicine [5], [6], intelligent logistics [7], [8], and 3D printing [9], [10]. In those sophisticated applications, the high-precision control of Delta parallel robot has become a critical issue for the researchers.

In the early works [11]–[13], the kinematic control method (the control designs based on the kinematic model) is proposed for the Delta parallel robot, which has been widely used in the present industry. It is easy to realize but may loose the accuracy in high speed and heavy load conditions. With the increase of speed and load, there arise some challenges: the dynamics of the Delta parallel robot, consisting the high nonlinearity and coupling, could inevitably influence the system performance; the presence of uncertainties such as, the residual vibration caused by the effect of the lightweight parallelogram, the uncertain system parameters with the random external load and the imperfectly known inputs, can not be ignored in the control design. Hence, there emerge a series of dynamic model based control strategies for the uncertain Delta parallel robot. An adaptive disturbance rejection control scheme for a 3-DOF Delta parallel robot is established to compensate a set of uncertainties in [14]. A LQR control strategy based on the pole placement and state feedback is proposed to diminish the external disturbances in [15]. In [16], a H_∞ controller can ensure the trajectory accuracy of a 3-DOF Delta parallel robot in the high speed

The associate editor coordinating the review of this manuscript and approving it for publication was Jun Shen.

operation. Reference [17] combined Type-1 and Type-2 fuzzy logic controller to manage different amplitudes of the injected noise and the inherent uncertainties of Delta parallel robot. The accuracy and robustness of the most present control approaches rely on the knowledge of the uncertainty (such as, [14]–[16]), which depend on the results of the numerous experiments for the uncertain Delta parallel robot.

In this paper, we devote to develop a new class of robust control by considering the imperfect knowledge of the uncertainty. The uncertainty considered in this paper includes the unknown dynamic parameters, the random residual vibration, and the non-structured portion of the nonlinear joints friction model, which are bounded but the exact bounds of those uncertain terms are unknown. Based on the Leitmann method [18]–[21] (a general deterministic control approach for the uncertain systems), two novel controllers merging the fractional robust control design and the online estimation for uncertainty are proposed to handle the strong nonlinearity of the uncertain Delta robot with joints friction.

There are three major contributions. First, the motion equation of the uncertain Delta parallel robot with nonlinear joints friction (caused by the effects of viscous, Coulomb and Stribeck friction) is constructed. The typical uncertainties of the Delta parallel robot in work condition are analyzed. Especially, the coupling issue of the active joints friction and the control torques is discussed and modeled as an uncertainty, which is often simplified by the linearization decoupling method in many applications. Second, two novel robust controls with online estimation for the Delta parallel robot are proposed. Both controls contain a model based friction compensation and a precise trajectory tracking scheme. The first control can guarantee the Delta parallel robot the deterministic performance (such as, uniform boundedness and uniform ultimate boundedness). The second control could not only ensure the same deterministic performance but also reduce the control cost by a high-order fractional stabilization design. Third, a new online estimation mechanism with exponential leakage term and dead-zone is proposed, which is nonlinear and performance dependent. It could generate a series of adaptive parameters to estimate the realtime uncertainties. The dead-zone design can simplify the estimation mechanism and the leakage term will decrease the control cost with the reduction of control system error.

II. THE UNCERTAIN DELTA PARALLEL ROBOT WITH JOINTS FRICTION

A. THE INVERSE KINEMATIC ANALYSIS OF THE DELTA PARALLEL ROBOT

Consider a typical three DOF Delta parallel robot in Fig. 1. It is comprised of the fixed platform, the moving platform and three kinematic chains connected by the end effector fixed on the moving platform. Each kinematic chain includes an active arm and a passive arm. The active arms of robot are driven by the rotational (DC or AC servo) actuators and attached to the passive arms. With the parallelogram-based structure of the passive arms, the moving platform can generate three purely translational motions.

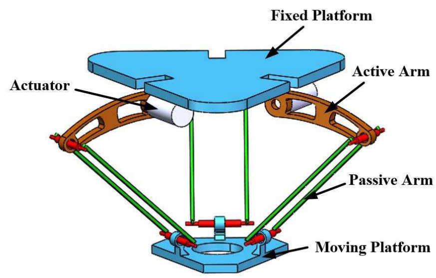

FIGURE 1. The Delta parallel robot.

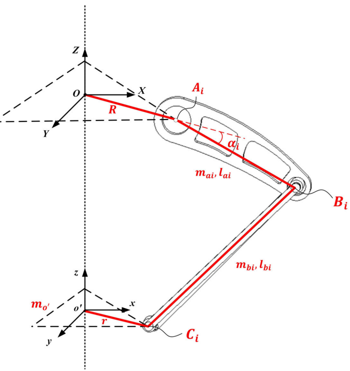

FIGURE 2. The parameters of the *i*-th kinematic chain.

Assign a base frame $\{O\}$ to the fixed platform and a local frame $\{o'\}$ to the moving platform in Fig. 2. Denote the parameters of the Delta parallel robot as follows ($i = 1, 2, 3$):

α_i–angle of the i-th active joint;
m_{ai}–mass of the i-th active arm;
m_{bi}–mass of the i-th passive arm;
$m_{o'}$–mass of the moving platform;
R–radius of the fixed platform;
r–radius of the moving platform;
l_{ai}–length of the i-th active arm;
l_{bi}–length of the i-th passive arm.

For the robot control issue, the kinematic model is concerned to obtain the relationship between the motions of the end effector and the active joints. In order to control the trajectory tracking error of the end effector, the inverse kinematic problem is proposed to investigate the control algorithms of the active joints in the following. Notice that there exist three identical kinematic chains (the closed loop form) for the Delta parallel robot. The closed loop for the i-th kinematic chain in Fig. 2 can be expressed as

$$\overrightarrow{B_iC_i} = \overrightarrow{Oo'} - \left(\overrightarrow{OA_i} + \overrightarrow{A_iB_i} + \overrightarrow{o'C_i}\right), \tag{1}$$

where A_i, B_i and C_i are the positions of the revolute joints relative to the base frame $\{O\}$, $i = 1, 2, 3$, and the coordinates are given by

$$A_i = \left[R\cos\varphi_i, R\sin\varphi_i, 0\right]^T, \tag{2}$$

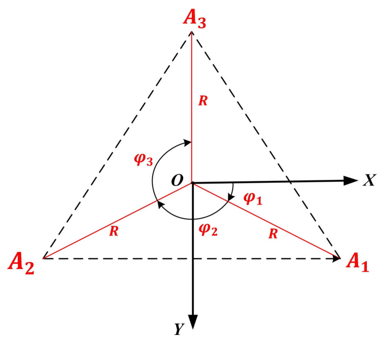

FIGURE 3. Distributions of A_i in the fixed platform.

$$B_i = \begin{bmatrix} (R + l_a \cos\alpha_i)\cos\varphi_i \\ (R + l_a \cos\alpha_i)\sin\varphi_i \\ -l_a \sin\alpha_i \end{bmatrix}, \quad (3)$$

$$C_i = \left[r\cos\varphi_i + x, r\sin\varphi_i + y, z\right]^T. \quad (4)$$

Here, $[x, y, z]^T$ represents the position of the local frame $\{o'\}$ relative to the base frame $\{O\}$, $\varphi_i = \left(\frac{2}{3}i - \frac{1}{2}\right)\pi$ is the angle between $\overrightarrow{OA_i}$ and X-axis (shown in Fig. 3, $i = 1, 2, 3$).

Recalling that $\left|\overrightarrow{B_iC_i}\right| = l_{bi}$, we can rewrite (1) as

$$[(R - r + l_{ai}\cos\alpha_i)\cos\varphi_i - x]^2 + [(R - r + l_{ai} \times \cos\alpha_i)\sin\varphi_i - y]^2 + [l_{ai}\sin\alpha_i + z]^2 = l_{bi}^2. \quad (5)$$

For the inverse kinematic problem, α_i can be determined by the explicit solution of the quadratic equation (5), $i = 1, 2, 3$.

Remark 1: When the position and orientation of the end-effector are determined, there exist two explicit solutions for each kinematic chain, which leads to 8 configurations of the Delta parallel robot. For a better performance, the configuration solution is chosen by $\|\alpha_i\| < \frac{\pi}{2}$, $i = 1, 2, 3$.

B. THE MOTION EQUATION OF THE UNCERTAIN DELTA PARALLEL ROBOT

Suppose $\alpha = [\alpha_1, \alpha_2, \alpha_3]^T$ is the generalized coordinate of the Delta parallel robot. Based on the dynamics constructed in [22], the motion equation of the Delta parallel robot with uncertainty can be formulated as

$$M(\alpha(t), \zeta(t), t)\ddot{\alpha}(t) + C(\alpha(t), \dot{\alpha}(t), \zeta(t), t)\dot{\alpha}(t) + G(\alpha(t), \zeta(t), t) + F(\alpha(t), \dot{\alpha}(t), \zeta(t), t) = \tau(t), \quad (6)$$

where $t \in R$ is the independent time variable, $\dot{\alpha} \in R^3$ is the velocity, $\ddot{\alpha} \in R^3$ is the acceleration, $\zeta \in \Xi \subset R^p$ is the uncertain parameter, $\tau(t) \in R^3$ is the control input applied by the driven motors. Here, $\Xi \in R^3$ is compact but unknown (standing for the possible bound of Ξ). Furthermore, $M(\alpha(t), \zeta(t), t)$ is the inertial matrix, $C(\alpha(t), \dot{\alpha}(t), \zeta(t), t)$ is the Coriolis/centrifugal force, $\dot{M}(\alpha(t), \zeta(t), t) - 2C(\alpha(t), \dot{\alpha}(t), \zeta(t), t)$ is the skew symmetric matrix, $G(\alpha(t), \zeta(t), t)$ is the gravitational force and $F(\alpha(t), \dot{\alpha}(t), \zeta(t), t)$ are the impressed force like the external disturbance. For simplicity, the arguments will be omitted without ambiguity. The detail expressions of $M(\cdot)$, $C(\cdot)$ and $G(\cdot)$ are

$$M = \left(\frac{1}{3}m_a l_a^2 + \frac{1}{2}m_b l_a^2\right) I + J^T\left(m_{o'} + \frac{3}{2}m_b\right) J, \quad (7)$$

$$C = J^T\left(m_{o'} + \frac{3}{2}m_b\right)\dot{J}, \quad (8)$$

$$G = \left(\frac{1}{2}m_a + \frac{1}{2}m_b\right) g l_a \begin{bmatrix} \cos\alpha_1 \\ \cos\alpha_2 \\ \cos\alpha_3 \end{bmatrix} - J^T\left(m_{o'} + \frac{3}{2}m_b\right)\begin{bmatrix} 0 \\ 0 \\ -g \end{bmatrix}, \quad (9)$$

where I is an identity matrix, J represents the Jacobian matrix which is

$$J = -\begin{bmatrix} s_1^T \\ s_2^T \\ s_3^T \end{bmatrix}^{-1}\begin{bmatrix} s_1^T b_1 & 0 & 0 \\ 0 & s_2^T b_2 & 0 \\ 0 & 0 & s_3^T b_3 \end{bmatrix}. \quad (10)$$

Here,

$$s_i = \begin{bmatrix} x \\ y \\ z \end{bmatrix} - {}_i^O R\left(\begin{bmatrix} R \\ 0 \\ 0 \end{bmatrix} + \begin{bmatrix} l_{ai}\cos\alpha_i \\ 0 \\ -l_{ai}\sin\alpha_i \end{bmatrix}\right),$$

$${}_i^O R = \begin{bmatrix} \cos\left(-\frac{\pi}{6} + \frac{2\pi}{3}i\right) & -\sin\left(-\frac{\pi}{6} + \frac{2\pi}{3}i\right) & 0 \\ \sin\left(-\frac{\pi}{6} + \frac{2\pi}{3}i\right) & \cos\left(-\frac{\pi}{6} + \frac{2\pi}{3}i\right) & 0 \\ 0 & 0 & 1 \end{bmatrix},$$

$$b_i = {}_i^O R\begin{bmatrix} l_{ai}\sin\alpha_i \\ 0 \\ l_{ai}\cos\alpha_i \end{bmatrix}, \quad i = 1, 2, 3.$$

Remark 2: There may exist several typical uncertainties of the Delta parallel robot in the high speed and heavy load condition. Firstly, the passive arms of the Delta parallel robot, made of lightweight slender rods, could lead to the residual vibration of the Delta parallel robot by the elastic deformation. It is considered as a high frequency and random external disturbance in the paper. Secondly, the mass of the moving platform with different loads in the high speed pick-and-place condition will be regarded as a fast time-varying uncertain parameter.

Hence, the dimension of the uncertain parameters vector $\zeta \in \Xi \subset R^p$ is determined by the number of the uncertain terms considered in the Delta parallel robot. Each of them is compact and bounded.

C. THE MOTION EQUATION OF THE UNCERTAIN DELTA PARALLEL ROBOT WITH JOINTS FRICTION

For a Delta parallel robot, the driven motors are assembled in the active joints, which give occasion to the coupling effects of the active joints friction and the control input torques [23]. Those coupling effects may influence the control accuracy and are considered as a difficulty in the friction compensation

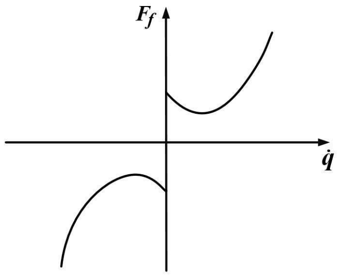

FIGURE 4. The Stribeck friction model.

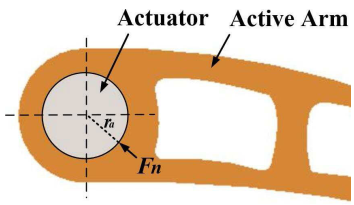

FIGURE 5. The normal force of the *i*-th active revolute joint.

control. Hence, in this paper, the friction of the active joints is discussed and modeled for the next control designs.

A Stribeck friction model, which can depict the viscous friction and the discontinuity from stiction to friction of the active joints in low-speed motion, is used to model the joints friction of the Delta parallel robot, see in Fig. 3, and the model is given by [24]

$$\begin{aligned} F_f &= \left[F_c + (F_s - F_c)e^{-(\frac{v}{v_s})^2}\right]\operatorname{sgn}(v) + \mu_v v, \\ F_c &= \mu_d F_n, \quad F_s = \mu_s F_n, \end{aligned} \tag{11}$$

where F_f is the Stribeck friction, F_c is Coulomb friction, F_s is the stiction friction, v is the relative velocity of the two contact objects, v_s is Stribeck velocity, μ_v is the coefficient of the viscous friction, μ_d is the coefficient of Coulomb friction, F_n is the normal force, μ_s is the coefficient of static friction.

By the Stribeck friction model in (11), the frictional moment of the i-th active joint can be expressed as

$$\begin{aligned} M_{fi} &= \left[F_{ci} + (F_{si} - F_{ci})e^{-(\frac{\dot{\alpha}_i}{v_{is}})^2}\right]\operatorname{sgn}(\dot{\alpha}_i)r_a + \mu_v\dot{\alpha}_i r_a, \\ F_{ci} &= \mu_d F_{ni}, \quad F_{si} = \mu_s F_{ni}, \end{aligned} \tag{12}$$

where F_{ni} is the normal force of the i-th active joint shown in Fig. 4, r_a is the friction arm of the active joints. Then the motion equation of the Delta parallel robot with uncertainty and joints friction can be deduced as

$$\begin{aligned} &M(\alpha,\zeta,t)\ddot{\alpha} + C(\alpha,\dot{\alpha},\zeta,t)\dot{\alpha} + G(\alpha,\zeta,t) \\ &\quad + F(\alpha,\dot{\alpha},\zeta,t) + M_f(\alpha,\dot{\alpha},\zeta,t) = \tau, \end{aligned} \tag{13}$$

where $M_f(\alpha,\dot{\alpha},\zeta,t) = \left[M_{f1}, M_{f2}, M_{f3}\right]^T$ represents the joints friction of the Delta parallel robot.

Remark 3: The joints friction in (11) contains two kinds of uncertain factors. The first kind of uncertainty is the time-varying friction coefficients, such as the viscous friction coefficient μ_v which is sensitive to the real-time temperature of the joints lubrication. The normal force F_n, produced by the constraints on the joint, is considered as the other uncertainty in the paper. The analytical form of the normal force, derived by Newtonian or Lagrangian approaches, is complicated and coupled with the control torque. In many applications, the normal force is assumed to be a constant, which may 'help' to decouple the normal force and the control input. While, the simplification could lead to the loss of the accuracy of the friction compensation control. Therefore, we model the normal force in the paper as an uncertainty with a certain bound.

III. THE ROBUST CONTROL DESIGN

Assume the planning trajectory of the Delta parallel robot is $\alpha^d(t), t \in [t_0, t_1]$, the desired velocity is $\dot{\alpha}^d(t)$ and the desired acceleration is $\ddot{\alpha}^d(t)$. Assume $\alpha^d(\cdot) : [t_0, \infty] \to R^3$ is of class C^2 and $\alpha^d(t)$, $\dot{\alpha}^d(t)$ and $\ddot{\alpha}^d(t)$ (uniformly bounded). Let

$$r(t) = \alpha(t) - \alpha^d(t), \tag{14}$$

and hence $\dot{r} = \dot{\alpha}(t) - \dot{\alpha}^d(t)$, $\ddot{r} = \ddot{\alpha}(t) - \ddot{\alpha}^d(t)$. The trajectory tracking error can be defined as:

$$\underline{r}(t) = \begin{bmatrix} r^T(t) & \dot{r}^T(t) \end{bmatrix}^T. \tag{15}$$

Decompose the M, C, G, F and M_f of the Delta parallel robot (13) as follows:

$$\begin{aligned} M(\alpha,\zeta,t) &= \bar{M}(\alpha,t) + \Delta M(\alpha,\zeta,t), && (16)\\ C(\alpha,\dot{\alpha},\zeta,t) &= \bar{C}(\alpha,\dot{\alpha},t) + \Delta C(\alpha,\dot{\alpha},\zeta,t), && (17)\\ G(\alpha,\zeta,t) &= \bar{G}(\alpha,t) + \Delta G(\alpha,\zeta,t), && (18)\\ F(\alpha,\dot{\alpha},\zeta,t) &= \bar{F}(\alpha,\dot{\alpha},t) + \Delta F(\alpha,\dot{\alpha},\zeta,t), && (19)\\ M_f(\alpha,\dot{\alpha},\zeta,t) &= \bar{M}_f(\alpha,\dot{\alpha},t) + \Delta M_f(\alpha,\dot{\alpha},\zeta,t). && (20) \end{aligned}$$

Here $\bar{M}$, $\bar{C}$, $\bar{G}$, $\bar{F}$ and $\bar{M}_f$ denote the "norm" portions with $\bar{M} > 0$ which is always practicable by the designer's decision, while ΔM, ΔC, ΔG, ΔF and ΔM_f are the uncertain portions. The functions $\bar{M}(\cdot)$, $\Delta M(\cdot)$, $\bar{C}(\cdot)$, $\Delta C(\cdot)$, $\bar{G}(\cdot)$, $\Delta G(\cdot)$, $\bar{F}(\cdot)$, $\Delta F(\cdot)$, $\bar{M}_f(\cdot)$ $\Delta M_f(\cdot)$ are all continuous.

Assumption 1: We assume that the inertia matrix $M(\alpha,\zeta,t)$ is uniformly positive definite, that is, there exists a scalar constant $\psi > 0$ such that

$$M(\alpha,\zeta,t) > \psi I. \tag{21}$$

Remark 4: In the past, the assumption of the uniformly positive definiteness of the inertia matrix $M(\alpha,\zeta,t)$ is often believed to be true rather than an assumption. The inertial matrix, however, is not always positive definitive in all mechanical systems. There are some counter examples listed in [25].

Assumption 2: For each $(\alpha, t) \in R^3 \times R$, $\zeta \in \Xi$, there exist constants $\kappa_j, j = 0, 1, 2$, with $\kappa_0 > 0$, $\kappa_{1,2} \geq 0$, such that

$$\|M(\alpha,\zeta,t)\| \leq \kappa_0 + \kappa_1\|\alpha\| + \kappa_2\|\alpha\|^2. \tag{22}$$

Remark 5: For any rigid serial type robots with revolute and slide joints, $M(\alpha,\zeta,t)$ is related to the parameters of the inertia matrix and the positions of the joints, which means there exists a set of constants κ_j such that for all $(\alpha, t) \in R^3 \times R$, $\zeta \in \Xi$, the euclidean norm of the inertia matrix satisfies (22).

A. THE ROBUST CONTROL DESIGN I

By the inverse dynamics, we propose a nominal control portion as:

$$C_1(\alpha(t), \dot{\alpha}(t), t) = \bar{M}(\alpha, t)\left(\ddot{\alpha}^d - D\dot{r}\right) + \bar{C}(\alpha, \dot{\alpha}, t) \times \left(\dot{\alpha}^d - Dr\right) + \bar{G}(\alpha, t) + \bar{F}(\alpha, \dot{\alpha}, t) + \bar{M}_f(\alpha, \dot{\alpha}, t), \quad (23)$$

where $D = \text{diag}[d_i]_{3\times 3}$, $d_i > 0$, $i = 1, 2, 3$.

Remark 6: The nominal control portion C_1 is designed by the information of the exact model, that is, one could apply the control input $\tau = C_1$ to drive the Delta parallel robot to track the desired trajectory when there is no initial condition deviation and the uncertainty.

Considering the inevitable initial deviation of the Delta parallel robot, we propose a P.D. control portion C_2 as

$$C_2(\alpha(t), \dot{\alpha}(t), t) = -T_p r - T_v \dot{r}, \quad (26)$$

here, $T_p = \text{diag}[t_{pi}]$, $t_{pi} > 0$, $T_v = \text{diag}[t_{vi}]$, $t_{vi} > 0$, $i = 1, 2, 3$.

Assumption 3: (1) For a given $D = \text{diag}[d_i]_{3\times 3}$, $d_i > 0$, $d_s = \lambda_{\min}(D)$, $i = 1, 2, 3$, there exists a (possibly unknown) constant vector $\rho \in (0, \infty)^k$ and a known function $\Lambda(\cdot) : (0, \infty)^k \times R^3 \times R^3 \times R \to R_+$ such that for all $(\alpha, \dot{\alpha}, t) \in R^3 \times R^3 \times R$, $\zeta \in \Xi$,

$$\|\eta(r, \dot{r}, \zeta, t)\| \le \Lambda(\rho, \alpha, \dot{\alpha}, t), \quad (27)$$

where

$$\eta(r, \dot{r}, \zeta, t) = -\Delta M(\alpha, \zeta, t)\left(\ddot{\alpha}^d - D\dot{r}\right) - \Delta C(\alpha, \dot{\alpha}, \zeta, t)\left(\dot{\alpha}^d - Dr\right) - \Delta G(\alpha, \zeta, t) - \Delta F(\alpha, \dot{\alpha}, \zeta, t) - \Delta M_f(\alpha, \dot{\alpha}, \zeta, t). \quad (28)$$

(2) For each $(\alpha, \dot{\alpha}, t) \in R^3 \times R^3 \times R$, the function $\Lambda(\cdot, \alpha, \dot{\alpha}, t)$ is: (*i*) C^1, (*ii*) a concave function of ρ; that is, for any ρ_1, ρ_2,

$$\Lambda(\rho_1, \alpha, \dot{\alpha}, t) - \Gamma(\rho_2, \alpha, \dot{\alpha}, t) \le \frac{\partial \Lambda}{\partial \rho}(\rho_2, \alpha, \dot{\alpha}, t)(\rho_1 - \rho_2). \quad (29)$$

(3) The function $\Lambda(\cdot, \alpha, \dot{\alpha}, t)$ is nondecreasing with respect to each component of its argument ρ.

Remark 7: The constant vector ρ is unknown since it may relate to the bounding set Ξ. The function Λ is treated as the upper bound of uncertainty. In the special case, when there is no uncertainty, $\Lambda = 0$.

Consider the following adaptive law with leakage term and dead-zone in (24)-(25), as shown at the bottom of this page.

Here, $\hat{\rho}_i(t_0) > 0$ ($\hat{\rho}_i$ is the ith component of the vector $\hat{\rho}$, $i = 1, 2, \ldots, k$), $b_1, b_2, b_3 \in R^{k\times k}$, each entry of b_1, b_2 and b_3 is non-negative, $\beta \in R$, $\beta > 0$, $\epsilon \in R$, $\epsilon > 0$.

Remark 8: The adaptive law (24)-(25) is designed to mimic the bound of uncertainty ρ ($\hat{\rho}$ represents the estimated value of ρ), which possesses two types: the leakage term and the dead-zone. The first term on the right-hand side of (24) is always nonnegative, and the second term on the is the leakage term which is designed to make $\hat{\rho}$ render an exponentially decaying to zero. Note that if the initial condition $\rho_i(t_0)$ is chosen to be strictly positive, then $\rho_i(t) > 0$ for all $t > t_0$, $i = 1, 2, \ldots, k$. The dead-zone portion (25) is actually an option, when it combines with (24), the adaptive law will simplify the calculation and the algorithm.

By Assumption 3 and the adaptive law (24)-(25), we propose an adaptive robust control portion C_3 as

$$C_3(\hat{\rho}(t), \alpha(t), \dot{\alpha}(t), t) = \varphi(\hat{\rho}, \alpha, \dot{\alpha}, t)\omega(\hat{\rho}, \alpha, \dot{\alpha}, t) \times \Lambda(\hat{\rho}, \alpha, \dot{\alpha}, t), \quad (30)$$

where

$$\varphi(\hat{\rho}, \alpha, \dot{\alpha}, t) = \begin{cases} \dfrac{1}{\|\omega(\hat{\rho}, \alpha, \dot{\alpha}, t)\|}, & \|\omega(\hat{\rho}, \alpha, \dot{\alpha}, t)\| > \xi; \\ \dfrac{1}{\xi}, & \|\omega(\hat{\rho}, \alpha, \dot{\alpha}, t)\| \le \xi; \end{cases} \quad (31)$$

$$\omega\left(\hat{\rho}, \alpha, \dot{\alpha}, t\right) = (\dot{r} + Dr)\Lambda(\hat{\rho}, \alpha, \dot{\alpha}, t), \quad (32)$$

here, $\xi > 0$.

Combined the control portions C_1, C_2 and C_3, we propose the controller deign I of the Delta parallel robot as

$$\tau(t) = C_1(\alpha(t), \dot{\alpha}(t), t) + C_2(\alpha(t), \dot{\alpha}(t), t) + C_3\left(\hat{\rho}(t), \alpha(t), \dot{\alpha}(t), t\right). \quad (33)$$

The system performance under the control design I is analyzed by the following theorem.

Theorem 1: Let $\mu = \left[\dot{r}^T, r^T, (\hat{\rho} - \rho)^T\right]^T \in R^{6+k}$. Subject to Assumptions 1, 2 and 3, the control (33) for the Delta parallel robot (13) renders μ the following performance:

(*i*) Uniform boundedness: For any $y > 0$ with $\|\mu(t_0)\| \le y$, there exists a $d(y) > 0$ such that $\|\mu(t)\| \le d(y)$ for all $t \ge t_0$;

$$\dot{\hat{\rho}} = \begin{cases} \beta\left[b_1 \dfrac{\partial \Lambda^T}{\partial \rho}(\hat{\rho}, \alpha, \dot{\alpha}, t)\|\dot{r} + Dr\| - \left(b_2 e^{-\|\dot{r}+Dr\|} + b_3\right)\hat{\rho}\right], & \|\dot{r} + Dr\|\left\|\dfrac{\partial \Lambda}{\partial \rho}(\hat{\rho}, \alpha, \dot{\alpha}, t)\right\| > \epsilon; \quad (24) \\ -\beta\left(b_2 e^{-\|\dot{r}+Dr\|} + b_3\right)\hat{\rho}. & \|\dot{r} + Dr\|\left\|\dfrac{\partial \Gamma}{\partial \rho}(\hat{\rho}, \alpha, \dot{\alpha}, t)\right\| \le \epsilon; \quad (25) \end{cases}$$

(*ii*) Uniform ultimate boundedness: For any $y > 0$ with $\|\mu(t_0)\| \leq y$, there exists a $\underline{d} > 0$ such that $\|\mu(t)\| \leq \bar{d}$ for any $\bar{d} > \underline{d}$ as for all $t \geq t_0 + T(\bar{d}, y)$, where $T(\bar{d}, y) < \infty$.

Proof: Let the Lyapunov function candidate as

$$V = \frac{1}{2}(\dot{r} + Dr)^T M(\dot{r} + Dr) + \frac{1}{2} r^T (T_p + DT_v) r + \frac{1}{2}(\hat{\rho} - \rho)^T (\beta b_1)^{-1} (\hat{\rho} - \rho). \quad (34)$$

For a given uncertainty $\zeta(\cdot)$ and corresponding trajectory $\alpha(\cdot)$, $\dot{\alpha}(\cdot)$ and $\hat{\rho}(\cdot)$, the derivative of V is given by

$$\dot{V} = (\dot{r} + Dr)^T M(\ddot{r} + D\dot{r}) + \frac{1}{2}(\dot{r} + Dr)^T \dot{M} \times (\dot{r} + Dr) + r^T (T_p + DT_v)\dot{r} + (\hat{\rho} - \rho)^T (\beta b_1)^{-1} \dot{\hat{\rho}}. \quad (35)$$

For simplicity, arguments of functions are omitted when no confusions exists, except for a few critical ones.

Each term of (35) will be analyzed separately. First,

$$\begin{aligned}(\dot{r} + Dr)^T M (\ddot{r} + D\dot{r}) &= (\dot{r} + Dr)^T M \left(\ddot{\alpha} - \ddot{\alpha}^d + D\dot{r}\right) \\ &= (\dot{r} + Dr)^T \left(\tau - C\left(\dot{r} + \dot{\alpha}^d\right) - G - F - M_f - M\ddot{\alpha}^d + MD\dot{r}\right) \\ &= (\dot{r} + Dr)^T \Big(C_1 + C_2 + C_3 - \Delta M\left(\ddot{\alpha}^d - D\dot{r}\right) - \Delta C\left(\dot{\alpha}^d - Dr\right) - \Delta G - \Delta F - \Delta M_f - \bar{G} \\ &\quad - \bar{F} - \bar{M}_f - \bar{M}\left(\ddot{\alpha}^d - D\dot{r}\right) - \bar{C}\left(\dot{\alpha}^d - Dr\right) - C(\dot{r} + Dr)\Big). \end{aligned} \quad (36)$$

Considering the design of C_1, we can get

$$(\dot{r} + Dr)^T \left(C_1 - \bar{M}\left(\ddot{\alpha}^d - D\dot{r}\right) - \bar{C}\left(\dot{\alpha}^d - Dr\right) - \bar{G} - \bar{F} - \bar{M}_f\right) = 0. \quad (37)$$

By the design of C_2, we have

$$\begin{aligned}(\dot{r} + Dr)^T C_2 &= -(\dot{r} + Dr)^T \left(-T_p r - T_v \dot{r}\right) \\ &= -\dot{r}^T T_p r - r^T DT_v \dot{r} - r^T DT_p r - \dot{r}^T T_v \dot{r}. \end{aligned} \quad (38)$$

By (32), we have

$$\begin{aligned}(\dot{r} + Dr)^T C_3 &= -(\dot{r} + Dr)^T \varphi\omega\Lambda\left(\hat{\rho}, \alpha, \dot{\alpha}, t\right) \\ &= -(\dot{r} + Dr)^T \varphi(\dot{r} + Dr)\Lambda^2\left(\hat{\rho}, \alpha, \dot{\alpha}, t\right) \\ &\leq -\varphi\|\omega\|^2. \end{aligned} \quad (39)$$

In (35), by Assumption 3, we have

$$\begin{aligned}&(\dot{r} + Dr)^T \left(-\Delta M\left(\ddot{\alpha}^d - D\dot{r}\right) - \Delta C\left(\dot{\alpha}^d - Dr\right) - \Delta G - \Delta F - \Delta M_f\right) \\ &\leq \|\dot{r} + Dr\| \left\|-\Delta M\left(\ddot{\alpha}^d - D\dot{r}\right) - \Delta C\left(\dot{\alpha}^d - Dr\right) - \Delta G - \Delta F - \Delta M_f\right\| \\ &\leq \|\dot{r} + Dr\| \Lambda(\rho, \alpha, \dot{\alpha}, t). \end{aligned} \quad (40)$$

The derivative of the Lyapunov function is

$$\begin{aligned}\dot{V} &= (\dot{r} + Dr)^T M(\ddot{r} + D\dot{r}) + \frac{1}{2}(\dot{r} + Dr)^T \dot{M} \times (\dot{r} + Dr) + r^T (T_p + DT_v)\dot{r} + (\hat{\rho} - \rho)^T (\beta b_1)^{-1} \dot{\hat{\rho}} \\ &\leq -\dot{r}^T T_v \dot{r} - r^T DT_p r + \|\dot{r} + Dr\| \Lambda(\rho, \alpha, \dot{\alpha}, t) - \varphi\|\omega\|^2 + (\hat{\rho} - \rho)^T (\beta b_1)^{-1} \dot{\hat{\rho}} \\ &\quad + \frac{1}{2}(\dot{r} + Dr)^T \left(\overbrace{\dot{M} - 2C}^{=0}\right)(\dot{r} + Dr) \\ &\leq -\lambda_v\|\dot{r}\|^2 - \lambda_{Dp}\|r\|^2 + \|\dot{r} + Dr\| \Lambda(\rho, \alpha, \dot{\alpha}, t) - \varphi\|\omega\|^2 + (\hat{\rho} - \rho)^T (\beta b_1)^{-1} \dot{\hat{\rho}}, \end{aligned} \quad (41)$$

where $\lambda_v = \lambda_{\min}(T_v)$, $\lambda_{Dp} = \lambda_{\min}(DT_p)$.

Considering the dead-zone conditions of the adaptive law in (24)-(25) and the robust gain design condition in (31), we will consider four possible cases.

Caes I: If $\|\dot{r} + Dr\| \left\|\frac{\partial \Lambda}{\partial \rho}(\hat{\rho}, \alpha, \dot{\alpha}, t)\right\| > \epsilon$ and $\|\omega(\hat{\rho}, \alpha, \dot{\alpha}, t)\| > \xi$, we have

$$\begin{aligned}\dot{V} &\leq -\lambda_v\|\dot{r}\|^2 - \lambda_{Dp}\|r\|^2 + \|\dot{r} + Dr\| \Lambda(\rho, \alpha, \dot{\alpha}, t) - \frac{1}{\|\omega\|}\|\omega\|^2 + (\hat{\rho} - \rho)^T b_1^{-1}\Big[b_1 \frac{\partial \Lambda^T}{\partial \rho}(\hat{\rho}, \alpha, \dot{\alpha}, t) \\ &\quad \times \|\dot{r} + Dr\| - \left(b_2 e^{-\|\dot{r} + Dr\|} + b_3\right)\hat{\rho}\Big] \\ &\leq -\lambda_v\|\dot{r}\|^2 - \lambda_{Dp}\|r\|^2 + \|\dot{r} + Dr\| \Lambda(\rho, \alpha, \dot{\alpha}, t) - \|\omega\| + (\hat{\rho} - \rho)^T b_1^{-1}\Big[b_1 \frac{\partial \Lambda^T}{\partial \rho}(\hat{\rho}, \alpha, \dot{\alpha}, t) \\ &\quad \times \|\dot{r} + Dr\| - \left(b_2 e^{-\|\dot{r} + Dr\|} + b_3\right)\hat{\rho}\Big] \\ &\leq -\lambda_v\|\dot{r}\|^2 - \lambda_{Dp}\|r\|^2 + \|\dot{r} + Dr\| \Lambda(\rho, \alpha, \dot{\alpha}, t) - \|\dot{r} + Dr\| \Lambda(\hat{\rho}, \alpha, \dot{\alpha}, t) + (\hat{\rho} - \rho)^T b_1^{-1} \\ &\quad \times \Big[b_1 \frac{\partial \Lambda^T}{\partial \rho}(\hat{\rho}, \alpha, \dot{\alpha}, t)\|\dot{r} + Dr\| - \left(b_2 e^{-\|\dot{r} + Dr\|} + b_3\right)\hat{\rho}\Big] \\ &\leq -\lambda_v\|\dot{r}\|^2 - \lambda_{Dp}\|r\|^2 + \|\dot{r} + Dr\| \frac{\partial \Lambda}{\partial \rho}(\hat{\rho}, \alpha, \dot{\alpha}, t) \\ &\quad \times (\rho - \hat{\rho}) + (\hat{\rho} - \rho)^T \frac{\partial \Lambda^T}{\partial \rho}(\hat{\rho}, \alpha, \dot{\alpha}, t)\|\dot{r} + Dr\| - (\hat{\rho} - \rho)^T b_1^{-1}\left(b_2 e^{-\|\dot{r} + Dr\|} + b_3\right)\hat{\rho} \\ &\leq -\lambda_v\|\dot{r}\|^2 - \lambda_{Dp}\|r\|^2 - (\hat{\rho} - \rho)^T b_1^{-1} \times \left(b_2 e^{-\|\dot{r} + Dr\|} + b_3\right)\left(\hat{\rho}\overbrace{-\rho + \rho}^{=0}\right) \\ &\leq -\lambda_v\|\dot{r}\|^2 - \lambda_{Dp}\|r\|^2 - b_1^{-1}\left(b_2 e^{-\|\dot{r} + Dr\|} + b_3\right) \times \left(\|\hat{\rho} - \rho\|^2 + \|\hat{\rho} - \rho\|\|\rho\|\right). \end{aligned} \quad (42)$$

According to the inequality $-ab \leq \frac{1}{2}\left(a^2+b^2\right)$, we have

$$
\begin{aligned}
-&\left(\|\hat{\rho}-\rho\|^2+\|\hat{\rho}-\rho\|\|\rho\|\right) \\
&\leq -\|\hat{\rho}-\rho\|^2+\frac{1}{2}\left(\|\rho\|^2+\|\hat{\rho}-\rho\|^2\right) \\
&\leq -\frac{1}{2}\|\hat{\rho}-\rho\|^2+\frac{1}{2}\|\rho\|^2, \qquad (43)
\end{aligned}
$$

then the third part of the equation (42) can be simplified as

$$
\begin{aligned}
-&b_1^{-1}\left(b_2 e^{-\|\dot{r}+Dr\|}+b_3\right)\left(\|\hat{\rho}-\rho\|^2+\|\hat{\rho}-\rho\|\|\rho\|\right) \\
&\leq b_1^{-1}\left(b_2 e^{-\|\dot{r}+Dr\|}+b_3\right)\left(-\frac{1}{2}\|\hat{\rho}-\rho\|^2+\frac{1}{2}\|\rho\|^2\right) \\
&\leq -\frac{1}{2}b_1^{-1}\left(b_2 e^{-\|\dot{r}+Dr\|}+b_3\right)\|\hat{\rho}-\rho\|^2 \\
&\quad +\frac{1}{2}b_1^{-1}\left(b_2 e^{-\|\dot{r}+Dr\|}+b_3\right)\|\rho\|^2. \qquad (44)
\end{aligned}
$$

Recalling that $\|\mu\|^2=\|\dot{r}\|^2+\|r\|^2+\|\hat{\rho}-\rho\|^2$, we can get

$$
\begin{aligned}
\dot{V} &\leq -\lambda_v\|\dot{r}\|^2-\lambda_{Dp}\|r\|^2-b_1^{-1}\left(b_2 e^{-\|\dot{r}+Dr\|}+b_3\right) \\
&\quad \times\left(\|\hat{\rho}-\rho\|^2+\|\hat{\rho}-\rho\|\|\rho\|\right) \\
&\leq -\lambda_v\|\dot{r}\|^2-\lambda_{Dp}\|r\|^2-\frac{1}{2}b_1^{-1}\left(b_2 e^{-\|\dot{r}+Dr\|}+b_3\right) \\
&\quad \|\hat{\rho}-\rho\|^2+\frac{1}{2}b_1^{-1}\left(b_2 e^{-\|\dot{r}+Dr\|}+b_3\right)\|\rho\|^2 \\
&\leq -\lambda_v\|\dot{r}\|^2-\lambda_{Dp}\|r\|^2-\frac{1}{2}b_1^{-1}\left(b_2+b_3\right)\|\hat{\rho}-\rho\|^2 \\
&\quad +\frac{1}{2}b_1^{-1}\left(b_2+b_3\right)\|\rho\|^2 \\
&\leq -\gamma_1\|\mu\|^2+\gamma_3, \qquad (45)
\end{aligned}
$$

where $\gamma_1 = \min\left\{\lambda_v, \lambda_{Dp}, \frac{1}{2}b_1^{-1}(b_2+b_3)\right\}$, $\gamma_3 = \frac{1}{2}b_1^{-1}\left(b_2+b_3\right)\|\rho\|^2$.

Case II: If $\|\dot{r}+Dr\|\left\|\frac{\partial\Lambda}{\partial\rho}(\hat{\rho},\alpha,\dot{\alpha},t)\right\| > \epsilon$ and $\|\omega(\hat{\rho},\alpha,\dot{\alpha},t)\| \leq \xi$, we can get

$$
\begin{aligned}
\dot{V} &\leq -\lambda_v\|\dot{r}\|^2-\lambda_{Dp}\|r\|^2+\|\dot{r}+Dr\|\,\Lambda(\rho,\alpha,\dot{\alpha},t) \\
&\quad -\frac{1}{\xi}\|\omega\|^2+(\hat{\rho}-\rho)^T(b_1)^{-1}\left[b_1\frac{\partial\Lambda^T}{\partial\rho}(\hat{\rho},\alpha,\dot{\alpha},t)\right. \\
&\quad \left.\times\|\dot{r}+Dr\|-\left(b_2 e^{-\|\dot{r}+Dr\|}+b_3\right)\hat{\rho}\right] \\
&\leq -\lambda_v\|\dot{r}\|^2-\lambda_{Dp}\|r\|^2+\|\dot{r}+Dr\|\,\Lambda(\rho,\alpha,\dot{\alpha},t) \\
&\quad \overbrace{-\|\dot{r}+Dr\|\,\Lambda(\hat{\rho},\alpha,\dot{\alpha},t)+\|\dot{r}+Dr\|\,\Lambda(\hat{\rho},\alpha,\dot{\alpha},t)}^{=0} \\
&\quad -\frac{1}{\xi}\|\omega\|^2+(\hat{\rho}-\rho)^T(b_1)^{-1}\left[b_1\frac{\partial\Lambda^T}{\partial\rho}(\hat{\rho},\alpha,\dot{\alpha},t)\right. \\
&\quad \left.\times\|\dot{r}+Dr\|-\left(b_2 e^{-\|\dot{r}+Dr\|}+b_3\right)\hat{\rho}\right] \\
&\leq -\lambda_v\|\dot{r}\|^2-\lambda_{Dp}\|r\|^2+\|\dot{r}+Dr\|\frac{\partial\Lambda}{\partial\rho}(\hat{\rho},\alpha,\dot{\alpha},t) \\
&\quad \times(\rho-\hat{\rho})+\|\dot{r}+Dr\|\,\Lambda(\hat{\rho},\alpha,\dot{\alpha},t) \\
&\quad -\frac{1}{\xi}\|\omega\|^2+(\hat{\rho}-\rho)^T\frac{\partial\Lambda^T}{\partial\rho}(\hat{\rho},\alpha,\dot{\alpha},t)\|\dot{r}+Dr\| \\
&\quad -(\hat{\rho}-\rho)^T b_1^{-1}\left(b_2 e^{-\|\dot{r}+Dr\|}+b_3\right)\hat{\rho} \\
&\leq -\lambda_v\|\dot{r}\|^2-\lambda_{Dp}\|r\|^2+\|\dot{r}+Dr\|\,\Lambda(\hat{\rho},\alpha,\dot{\alpha},t) \\
&\quad -\frac{1}{\xi}\|\omega\|^2-(\hat{\rho}-\rho)^T b_1^{-1}\left(b_2 e^{-\|\dot{r}+Dr\|}+b_3\right)\hat{\rho} \\
&\leq -\lambda_v\|\dot{r}\|^2-\lambda_{Dp}\|r\|^2+\frac{\xi}{4}-(\hat{\rho}-\rho)^T b_1^{-1} \\
&\quad \times\left(b_2 e^{-\|\dot{r}+Dr\|}+b_3\right)\left(\hat{\rho}\overbrace{-\rho+\rho}^{=0}\right) \\
&\leq -\lambda_v\|\dot{r}\|^2-\lambda_{Dp}\|r\|^2-\frac{1}{2}b_1^{-1}\left(b_2+b_3\right)\|\hat{\rho}-\rho\|^2 \\
&\quad +\frac{\xi}{4}+\frac{1}{2}b_1^{-1}\left(b_2+b_3\right)\|\rho\|^2 \\
&\leq -\gamma_1\|\mu\|^2+\gamma_4, \qquad (46)
\end{aligned}
$$

where $\gamma_1 = \min\left\{\lambda_v, \lambda_{Dp}, \frac{1}{2}b_1^{-1}\left(b_2+b_3\right)\right\}$, $\gamma_4 = \frac{\xi}{4}+\frac{1}{2}b_1^{-1}\left(b_2+b_3\right)\|\rho\|^2$.

Case III: If $\|\dot{r}+Dr\|\left\|\frac{\partial\Lambda}{\partial\rho}(\hat{\rho},\alpha,\dot{\alpha},t)\right\| \leq \epsilon$ and $\|\omega(\hat{\rho},\alpha,\dot{\alpha},t)\| > \xi$, we can rewrite as

$$
\begin{aligned}
\dot{V} &\leq -\lambda_v\|\dot{r}\|^2-\lambda_{Dp}\|r\|^2+\|\dot{r}+Dr\|\,\Lambda(\rho,\alpha,\dot{\alpha},t) \\
&\quad -\|\omega\|-(\hat{\rho}-\rho)^T b_1^{-1}\left(b_2 e^{-\|\dot{r}+Dr\|}+b_3\right)\hat{\rho} \\
&\leq -\lambda_v\|\dot{r}\|^2-\lambda_{Dp}\|r\|^2+\|\dot{r}+Dr\|\frac{\partial\Lambda}{\partial\rho}(\hat{\rho},\alpha,\dot{\alpha},t) \\
&\quad \times(\rho-\hat{\rho})-(\hat{\rho}-\rho)^T b_1^{-1}\left(b_2 e^{-\|\dot{r}+Dr\|}+b_3\right)\hat{\rho} \\
&\leq -\lambda_v\|\dot{r}\|^2-\lambda_{Dp}\|r\|^2+\epsilon\|\rho-\hat{\rho}\| \\
&\quad -(\hat{\rho}-\rho)^T b_1^{-1}\left(b_2 e^{-\|\dot{r}+Dr\|}+b_3\right)\left(\hat{\rho}\overbrace{-\rho+\rho}^{=0}\right) \\
&\leq -\lambda_v\|\dot{r}\|^2-\lambda_{Dp}\|r\|^2-\frac{1}{2}b_1^{-1}\left(b_2+b_3\right)\|\hat{\rho}-\rho\|^2 \\
&\quad +\epsilon\|\rho-\hat{\rho}\|+\frac{1}{2}b_1^{-1}\left(b_2+b_3\right)\|\rho\|^2 \\
&\leq -\gamma_1\|\mu\|^2+\gamma_2\|\mu\|+\gamma_3, \qquad (47)
\end{aligned}
$$

where $\gamma_2=\epsilon$.

Case IV: If $\|\dot{r}+Dr\|\left\|\frac{\partial\Lambda}{\partial\rho}(\hat{\rho},\alpha,\dot{\alpha},t)\right\| \leq \epsilon$ and $\|\omega(\hat{\rho},\alpha,\dot{\alpha},t)\| \leq \xi$, we have

$$
\begin{aligned}
\dot{V} &\leq -\lambda_v\|\dot{r}\|^2-\lambda_{Dp}\|r\|^2+\|\dot{r}+Dr\|\,\Lambda(\rho,\alpha,\dot{\alpha},t) \\
&\quad -\frac{1}{\xi}\|\omega\|^2-(\hat{\rho}-\rho)^T b_1^{-1}\left(b_2 e^{-\|\dot{r}+Dr\|}+b_3\right)\hat{\rho} \\
&\leq -\lambda_v\|\dot{r}\|^2-\lambda_{Dp}\|r\|^2+\|\dot{r}+Dr\|\frac{\partial\Lambda}{\partial\rho}(\hat{\rho},\alpha,\dot{\alpha},t) \\
&\quad \times(\rho-\hat{\rho})+\|\dot{r}+Dr\|\,\Lambda(\hat{\rho},\alpha,\dot{\alpha},t) \\
&\quad -\frac{1}{\xi}\|\omega\|^2-(\hat{\rho}-\rho)^T b_1^{-1}\left(b_2 e^{-\|\dot{r}+Dr\|}+b_3\right)\hat{\rho} \\
&\leq -\lambda_v\|\dot{r}\|^2-\lambda_{Dp}\|r\|^2+\epsilon\|\rho-\hat{\rho}\|+\frac{\xi}{4} \\
&\quad -b_1^{-1}\left(b_2 e^{-\|\dot{r}+Dr\|}+b_3\right)\left(\hat{\rho}\overbrace{-\rho+\rho}^{=0}\right)
\end{aligned}
$$

$$\leq -\lambda_v\|\dot{r}\|^2 - \lambda_{Dp}\|r\|^2 - \frac{1}{2}b_1^{-1}(b_2+b_3)\|\hat{\rho}-\rho\|^2 + \epsilon\|\rho-\hat{\rho}\| + \frac{\xi}{4} + \frac{1}{2}b_1^{-1}(b_2+b_3)\|\rho\|^2 \leq -\gamma_1\|\mu\|^2 + \gamma_2\|\mu\| + \gamma_4. \tag{48}$$

From the above results in (45), (46), (47) and (48), we formulate a general form of the inequation of the derivation of Lyapunov function as

$$\dot{V} \leq -\sigma_1\|\mu\|^2 + \sigma_2\|\mu\| + \sigma_3, \tag{49}$$

where $\sigma_1 = \gamma_1, \sigma_2 = \max\{\gamma_2, 0\}$ and $\sigma_3 = \max\{\gamma_3, \gamma_4\}$.

Upon invoking the standard arguments as in [26], we can conclude the uniform boundedness and the uniform ultimate boundedness with

$$d(y) = \begin{cases} \sqrt{\frac{\Phi_2}{\Phi_1}}Y, & \text{if} \quad y \leq Y; \\ \sqrt{\frac{\Phi_2}{\Phi_1}}y, & \text{if} \quad y > Y, \end{cases} \tag{50}$$

$$Y = \frac{1}{2\sigma_1}(\sigma_2 + \sqrt{\sigma_2^2 + 4\sigma_1\sigma_3}), \tag{51}$$

$$\underline{d} = \sqrt{\frac{\Phi_2}{\Phi_1}}Y, \tag{52}$$

and

$$T(\bar{d}, y) = \begin{cases} 0, & y \leq \bar{d}\sqrt{\frac{\Phi_2}{\Phi_1}}; \\ \dfrac{\Phi_2 y^2 - (\frac{\Phi_1^2}{\Phi_2})\bar{d}^2}{\sigma_1\bar{d}^2(\frac{\Phi_1}{\Phi_2}) - \sigma_2\bar{d}(\frac{\Phi_1}{\Phi_2}) - \sigma_3}, & y > \bar{d}\sqrt{\frac{\Phi_2}{\Phi_1}}; \end{cases} \tag{53}$$

where $\Phi_1 = \min\left\{\lambda_{\min}(M), (\beta b_1)^{-1}\right\}$,
$\Phi_2 = \max\left\{\lambda_{\max}(M), (\beta b_1)^{-1}\right\}$. ■

B. THE ROBUST CONTROL DESIGN II

Next, we introduce an alternative control design II as

$$\tau(t) = C_1(\alpha(t), \dot{\alpha}(t), t) + C_2(\alpha(t), \dot{\alpha}(t), t) + C_4\left(\hat{\rho}(t), \alpha(t), \dot{\alpha}(t), t\right), \tag{54}$$

where

$$C_4(\hat{\rho}(t), \alpha(t), \dot{\alpha}(t), t) = \varphi(\hat{\rho}, \alpha, \dot{\alpha}, t)\omega(\hat{\rho}, \alpha, \dot{\alpha}, t) \times \Lambda(\hat{\rho}, \alpha, \dot{\alpha}, t), \tag{55}$$

$$\varphi\left(\hat{\rho}, \alpha, \dot{\alpha}, t\right) = \frac{\|\omega\left(\hat{\rho}, \alpha, \dot{\alpha}, t\right)\|}{\|\omega\left(\hat{\rho}, \alpha, \dot{\alpha}, t\right)\|^2 + \|\omega\left(\hat{\rho}, \alpha, \dot{\alpha}, t\right)\|\xi + \xi^2}, \tag{56}$$

$$\omega\left(\hat{\rho}, \alpha, \dot{\alpha}, t\right) = (\dot{r} + Dr)\Lambda\left(\hat{\rho}, \alpha, \dot{\alpha}, t\right). \tag{57}$$

Remark 9: The robust gain $\varphi(\cdot)$ in (31) and (56) are fractional type. The robust gain $\varphi(\cdot)$ in (56) is intentionally proposed to reduce the control cost by the high order polynomial design. We can easily deduce that the robust gain $\varphi(\cdot)$ in (56) is always smaller than it in (31) for all $(\hat{\rho}, \alpha, \dot{\alpha}, t)$. It means that the control design II will have a lower control cost. While, as a trade-off, the control design II with the relatively complex robust gain design will consume more computation time. Then, in the future applications, the engineers could make a choice in the two control designs by the actual requirements of the robots.

Theorem 2: Let $\mu = \left[\dot{r}^T, r^T, (\hat{\rho} - \rho)^T\right]^T \in R^{6+k}$. Subject to Assumptions 1, 2 and 3, the control (54) renders δ the following performance:

(i) Uniform boundedness: For any $y > 0$ with $\|\mu(t_0)\| \leq y$, there exists a $d(y) > 0$ such that $\|\mu(t)\| \leq d(y)$ for all $t \geq t_0$;

(ii) Uniform ultimate boundedness: For any $y > 0$ with $\|\mu(t_0)\| \leq y$, there exists a $\underline{d} > 0$ such that $\|\mu(t)\| \leq \bar{d}$ for any $\bar{d} > \underline{d}$ as for all $t \geq t_0 + T(\bar{d}, y)$, where $T(\bar{d}, y) < \infty$.

Proof: Let

$$V = \frac{1}{2}(\dot{r} + Dr)^T M(\dot{r} + Dr) + \frac{1}{2}r^T(T_p + DT_v)r + \frac{1}{2}(\hat{\rho} - \rho)^T(\beta b_1)^{-1}(\hat{\rho} - \rho). \tag{58}$$

be the Lyapunov function candidate again. Then the derivative of V is given by

$$\dot{V} = (\dot{r}+Dr)^T M(\ddot{r}+D\dot{r}) + \frac{1}{2}(\dot{r}+Dr)^T\dot{M}(\dot{r}+Dr) + r^T(T_p + DT_v)\dot{r} + (\hat{\rho} - \rho)^T(\beta b_1)^{-1}\dot{\hat{\rho}} \leq -\lambda_v\|\dot{r}\|^2 - \lambda_{Dp}\|r\|^2 + \|\dot{r} + Dr\|\,\Lambda(\rho, \alpha, \dot{\alpha}, t) - \varphi\|\omega\|^2 + (\hat{\rho} - \rho)^T(\beta b_1)^{-1}\dot{\hat{\rho}}. \tag{59}$$

Considering the dead-zone conditions of the adaptive law in (24)-(25) and the robust gain design condition in (56), we will develop (59) under the two combinations of the inequalities.

If $\|\dot{r} + Dr\|\left\|\frac{\partial\Lambda}{\partial\rho}(\hat{\rho}, \alpha, \dot{\alpha}, t)\right\| > \epsilon$, we have

$$\begin{aligned}\dot{V} \leq\ & -\lambda_v\|\dot{r}\|^2 - \lambda_{Dp}\|r\|^2 + \|\dot{r} + Dr\|\,\Lambda(\rho, \alpha, \dot{\alpha}, t) - \frac{\|\omega\|}{\|\omega\|^2 + \|\omega\|\xi + \xi^2}\|\omega\|^2 + (\hat{\rho} - \rho)^T b_1^{-1} \\ & \times \left[b_1\frac{\partial\Lambda^T}{\partial\rho}(\hat{\rho}, \alpha, \dot{\alpha}, t)\|\dot{r} + Dr\| - \left(b_2 e^{-\|\dot{r}+Dr\|} + b_3\right)\hat{\rho}\right] \\ \leq\ & -\lambda_v\|\dot{r}\|^2 - \lambda_{Dp}\|r\|^2 + \|\dot{r} + Dr\|\,\Lambda(\rho, \alpha, \dot{\alpha}, t) - \|\omega\| + (\hat{\rho} - \rho)^T b_1^{-1}\left[b_1\frac{\partial\Lambda^T}{\partial\rho}(\hat{\rho}, \alpha, \dot{\alpha}, t)\right. \\ & \left. \times \|\dot{r} + Dr\| - \left(b_2 e^{-\|\dot{r}+Dr\|} + b_3\right)\hat{\rho}\right] \\ \leq\ & -\lambda_v\|\dot{r}\|^2 - \lambda_{Dp}\|r\|^2 + \|\dot{r} + Dr\|\frac{\partial\Lambda}{\partial\rho}(\hat{\rho}, \alpha, \dot{\alpha}, t) \\ & \times (\rho - \hat{\rho}) + (\hat{\rho} - \rho)^T\frac{\partial\Lambda^T}{\partial\rho}(\hat{\rho}, \alpha, \dot{\alpha}, t)\|\dot{r} + Dr\| \\ & - (\hat{\rho} - \rho)^T b_1^{-1}\left(b_2 e^{-\|\dot{r}+Dr\|} + b_3\right)\hat{\rho}\end{aligned}$$

$$
\begin{aligned}
&\leq -\lambda_v\|\dot r\|^2-\lambda_{Dp}\|r\|^2-b_1^{-1}\left(b_2e^{-\|\dot r+Dr\|}+b_3\right)\\
&\quad\times\left(\|\hat\rho-\rho\|^2+\|\hat\rho-\rho\|\|\rho\|\right)\\
&\leq -\lambda_v\|\dot r\|^2-\lambda_{Dp}\|r\|^2-\frac{1}{2}b_1^{-1}\left(b_2+b_3\right)\|\hat\rho-\rho\|^2\\
&\quad+\frac{1}{2}b_1^{-1}\left(b_2+b_3\right)\|\rho\|^2\\
&\leq -\gamma_1\|\mu\|^2+\gamma_3. \qquad (60)
\end{aligned}
$$

If $\|\dot r+Dr\|\left\|\frac{\partial\Lambda}{\partial\rho}(\hat\rho,\alpha,\dot\alpha,t)\right\|<\epsilon$, we have

$$
\begin{aligned}
\dot V&\leq -\lambda_v\|\dot r\|^2-\lambda_{Dp}\|r\|^2+\|\dot r+Dr\|\,\Lambda(\rho,\alpha,\dot\alpha,t)\\
&\quad-\frac{\|\omega\|}{\|\omega\|^2+\|\omega\|\xi+\xi^2}\|\omega\|^2\\
&\quad-(\hat\rho-\rho)^Tb_1^{-1}\left(b_2e^{-\|\dot r+Dr\|}+b_3\right)\hat\rho\\
&\leq -\lambda_v\|\dot r\|^2-\lambda_{Dp}\|r\|^2+\|\dot r+Dr\|\,\Lambda(\rho,\alpha,\dot\alpha,t)\\
&\quad-\|\omega\|-(\hat\rho-\rho)^Tb_1^{-1}\left(b_2e^{-\|\dot r+Dr\|}+b_3\right)\hat\rho\\
&\leq -\lambda_v\|\dot r\|^2-\lambda_{Dp}\|r\|^2+\|\dot r+Dr\|\frac{\partial\Lambda}{\partial\rho}(\hat\rho,\alpha,\dot\alpha,t)\\
&\quad\times(\rho-\hat\rho)-(\hat\rho-\rho)^Tb_1^{-1}\left(b_2e^{-\|\dot r+Dr\|}+b_3\right)\hat\rho\\
&\leq -\lambda_v\|\dot r\|^2-\lambda_{Dp}\|r\|^2+\epsilon\|\rho-\hat\rho\|\\
&\quad-(\hat\rho-\rho)^Tb_1^{-1}\beta\left(b_2e^{-\|\dot r+Dr\|}+b_3\right)\hat\rho\\
&\leq -\lambda_v\|\dot r\|^2-\lambda_{Dp}\|r\|^2+\epsilon\|\rho-\hat\rho\|\\
&\quad-\frac{1}{2}b_1^{-1}\left(b_2+b_3\right)\|\hat\rho-\rho\|^2\\
&\quad+\frac{1}{2}b_1^{-1}\left(b_2+b_3\right)\|\rho\|^2\\
&\leq -\gamma_1\|\mu\|^2+\gamma_2\|\delta\|+\gamma_3. \qquad (61)
\end{aligned}
$$

From the above results in (60) and (61), the inequation of the derivation of Lyapunov function can also be formulate by (49). Upon invoking the standard arguments as in [26], we conclude the uniform boundedness with

$$
d(y)=\begin{cases}\sqrt{\dfrac{\Phi_2}{\Phi_1}}Y, & if \quad y\leq Y;\\[2mm] \sqrt{\dfrac{\Phi_2}{\Phi_1}}y, & if \quad y>Y,\end{cases} \qquad (62)
$$

$$
Y=\frac{1}{2\gamma_1}(\gamma_2+\sqrt{\gamma_2^2+4\gamma_1\gamma_3}). \qquad (63)
$$

Furthermore, uniform ultimate boundedness also follows with

$$
\underline{d}=\sqrt{\frac{\Phi_2}{\Phi_1}}Y, \qquad (64)
$$

$$
T(\overline{d},y)=\begin{cases}0, & y\leq\overline{d}\sqrt{\dfrac{\Phi_2}{\Phi_1}};\\[2mm] \dfrac{\Phi_2y^2-(\frac{\Phi_1^2}{\Phi_2})\overline{d}^2}{\gamma_1\overline{d}^2(\frac{\Phi_1}{\Phi_2})-\gamma_2\overline{d}(\frac{\Phi_1}{\Phi_2})-\gamma_3}, & y>\overline{d}\sqrt{\dfrac{\Phi_2}{\Phi_1}};\end{cases} \qquad (65)
$$

where $\Phi_1=\min\left\{\lambda_{\min}(M),(\beta b_1)^{-1}\right\}$, $\Phi_2=\max\{\lambda_{\max}(M),(\beta b_1)^{-1}\}$. ■

TABLE 1. Parameters of the Delta parallel robot.

Description	Notation	Value	Units
Radius of the fixed platform	R	0.15	m
Radius of the moving platform	r	0.08	m
Length of the active arm	l_a	0.2	m
Length of the passive arm	l_b	0.4	m
Friction arm of the active arm	r_a	0.04	m
Mass of the active arm	m_a	0.2	Kg
Mass of the passive arm	m_b	0.2	Kg
Mass of the moving platform	$m_{o'}$	0.3	Kg
Stribeck velocity	v_s	0.1	rad/s
Gravity acceleration	g	9.8	m/seg^2
Coefficient of static friction	μ_s	0.2	
Coefficient of Coulomb friction	μ_d	0.1	
Coefficient of the viscous friction	μ_v	2	

IV. CONTROL DESIGN PROCEDURE

The control design procedure of the Delta parallel robot with uncertainty and joints friction can be summarized as follows:

Step 1: By (13), construct the motion equation of the uncertain Delta parallel robot with joints friction and decompose the motion equation into two parts: the nominal terms $\bar M$, $\bar C$, $\bar G$, $\bar F$ and $\bar M_f$; the uncertain terms ΔM, ΔC, ΔG, ΔF and ΔM_f;

Step 2: Check the Assumptions 1 and 2 for the Delta parallel robot and formulate the nominal control portion C_1 by (23); Choose the control parameter D by $D>0$.

Step 3: Deduce the trajectory tracking error and establish the P.D. control portion C_2 by (26); Choose the proportional control parameter $T_p>0$ and differential control parameter $T_v>0$.

Step 4: Derive the function $\Lambda(\cdot)$ by Assumption 3 and obtain the adaptive law in (24)-(25); Choose the online estimation sensitivity parameter $b_1>0$, dead-zone parameter $\epsilon>0$, leakage term parameters $b_2>0$ and $b_3>0$.

Step 5: According to the actual demands of the control system, formulate the corresponding robust control portion C_3 or C_4 by (30) or (55); Choose the robust gain $\beta>0$ and dead-zone parameter $\xi>0$.

Step 6: Construct the robust control design as $\tau=C_1+C_2+C_3$ or $\tau=C_1+C_2+C_4$ by the priority to the system performance or the efficiency of the control algorithm.

V. NUMERICAL SIMULATIONS

In this section, we consider a high speed 3-DOF Delta parallel robot with joints friction which is applied in intelligent logistics. The dynamic parameters of the Delta parallel robot in (13) are displayed in Table 1 according to [14].

In the working process, there are several typical uncertainties of the Delta parallel robot considered in the simulation: the changing mass of the moving platform $m_{o'}$ in the pick and place cycles; the time-varying normal force F_n of the joints friction; the external disturbance F caused by the vibration of the lightweight arms.

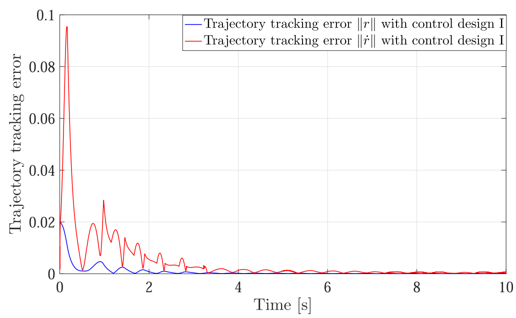

FIGURE 6. The trajectory tracking error under control design I.

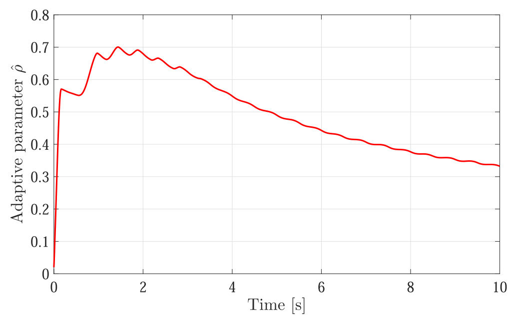

FIGURE 7. The time history of adaptive parameter $\hat{\rho}$ under control design I.

Those uncertainties can be expressed as: $m_{o'} = \bar{m}_{o'} + \Delta m_{o'}(t)$, $F_n = \bar{F}_n + \Delta F_n(t) = [\bar{F}_{n1}, \bar{F}_{n2}, \bar{F}_{n3}]^T + [\Delta F_{n1}(t), \Delta F_{n2}(t), \Delta F_{n3}(t)]^T$, and $F = \bar{F} + \Delta F(t) = [\bar{F}_1, \bar{F}_2, \bar{F}_3]^T + [\Delta F_1(t), \Delta F_2(t), \Delta F_3(t)]^T$. $\bar{m}_{o'}$, $\bar{F}_n$, and $\bar{F}$ are the nominal portions which are selected to be strictly positive, $\Delta m_{o'}(t)$, $\Delta F_n(t)$, and $\Delta F(t)$ are the time-varying uncertain portions. Then the uncertain parameter is chosen as $\zeta = [\Delta m_{o'}, \Delta F_{n1}, \Delta F_{n2}, \Delta F_{n3}, \Delta F_1, \Delta F_2, \Delta F_3]^T$.

Let $[x, y, z]^T$ stand for the coordinates of the end-effector of the Delta parallel robot. Suppose the desired trajectory (path type I) of robot be

$$\begin{bmatrix} x^d(t) \\ y^d(t) \\ z^d(t) \end{bmatrix} = \begin{bmatrix} 0.05t/15\cos(2\pi t) \\ 0.05t/15\sin(2\pi t) \\ -0.35 + 0.01t \end{bmatrix}. \quad (66)$$

Assumptions 1 and 2 are verified by the chosen $\bar{M}$. Note that the terms in M, C, and G are either constant, linear in positions, or quadratic in velocities, Assumption 3 can be met by choosing

$$\begin{aligned} \Lambda(\rho, \alpha, \dot{\alpha}, t) &= \rho_1\|\ddot{\alpha}^d - D\dot{r}\| + \rho_2\|\dot{\alpha}^d - Dr\| + \rho_3 \\ &\leq \rho\left(\|\ddot{\alpha}^d - D\dot{r}\| + \rho_2\|\dot{\alpha}^d - Dr\| + 1\right), \quad (67) \end{aligned}$$

where $\rho = \max\{\rho_1, \rho_2, \rho_3\}$.

For the simulation of the Delta parallel robot in MATLAB, the nominal values of the uncertain parameters are: $\bar{m}_{o'} = 0.3$kg, $\bar{F}_{ni} = 15$N, $\bar{F}_1 = 2$N, $\bar{F}_2 = 4$N and $\bar{F}_3 = 6$N, $i = 1, 2, 3$. Suppose the uncertain parameters are: $\Delta m_{o'} = \Delta_m \bar{m}_{o'} \sin(\pi t)$, $\Delta F_{ni} = \Delta_{fc}\bar{F}_{ni}\sin(\pi t)$, and $\Delta F_i = \Delta_f \bar{F}_i \cos(2\pi t)$, where $\Delta_m = \max_t \|\Delta m_{o'}(t)\|/\bar{m}_{o'}$, $\Delta_{fc} = \max_t \|\Delta F_{ni}(t)\|/\bar{F}_{ni}$, and $\Delta_f = \max_t \Delta F_i(t)/\bar{F}_i$, $i = 1, 2, 3$. Δ_m, Δ_{fc}, and Δ_f indicate the magnitude of the uncertainty which are all 0.3. Let the initial conditions are $\alpha_0 = [0.3322, 0.3322, 0.3322]^T$, $\dot{\alpha}_0 = [0, 0, 0]^T$, $\ddot{\alpha}_0 = [0, 0, 0]^T$, $\hat{\rho}_0 = 2$. Considering the system performance and the control cost, we choose the control parameters: $T_v = \text{diag}[9, 9, 9]$, $T_p = \text{diag}[3, 3, 3]$, $D = \text{diag}[9, 9, 9]$, $\beta = 0.1$ and $\xi = 0.001$. With a high sensitivity for the uncertainty, the online estimation parameters are chosen as follows: $\epsilon = 0.05$, $b_1 = 10$, $b_2 = 2$ and $b_3 = 0.3$. The simulation results are shown in Fig. 6-Fig. 22.

First, the simulation results under the adaptive robust control design I are shown in Fig. 6-Fig. 11. The trajectory tracking errors $\|r\|$ and $\|\dot{r}\|$ under control design I are shown in Fig. 6. The trajectory tracking error $\|r\|$ goes into a narrow zone around 0 after 0.3s and remains in it after, the error $\|\dot{r}\|$ increases at first and then approximately close to 0 after 3s. Fig. 7 shows the time history of the adaptive parameter $\hat{\rho}$.

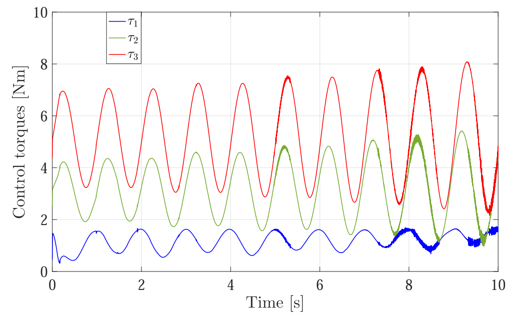

FIGURE 8. The time histories of the control inputs under control design I.

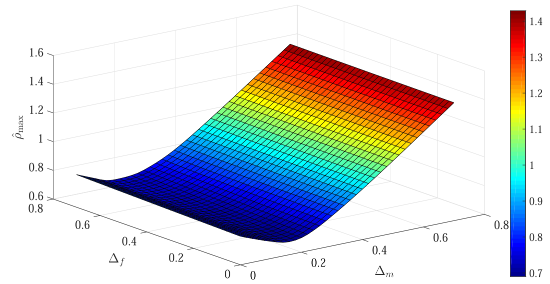

FIGURE 9. Maximum of $\hat{\rho}_{\max}$ with respect to Δ_m and Δ_f under control design I.

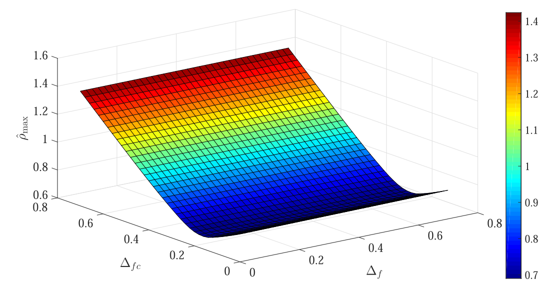

FIGURE 10. Maximum of $\hat{\rho}_{\max}$ with respect to Δ_f and Δ_{fc} under control design I.

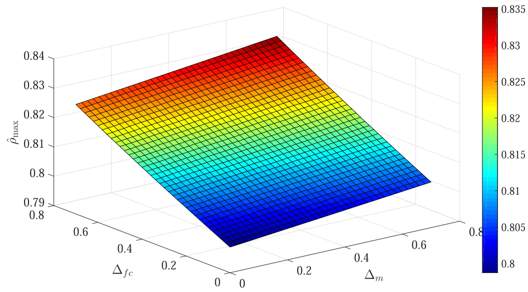

FIGURE 11. Maximum of $\hat{\rho}_{\max}$ with respect to Δ_m and Δ_{fc} under control design I.

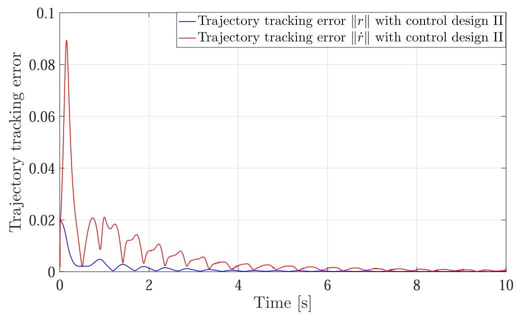

FIGURE 12. The trajectory tracking error under control design II.

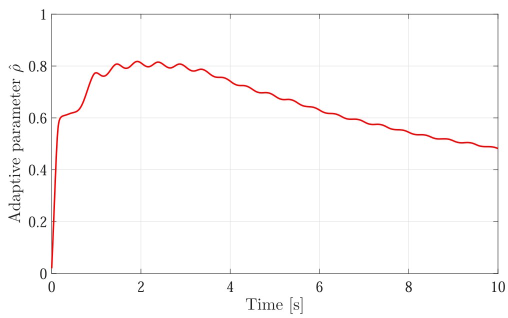

FIGURE 13. The time history of adaptive parameter $\hat{\rho}$ under control design II.

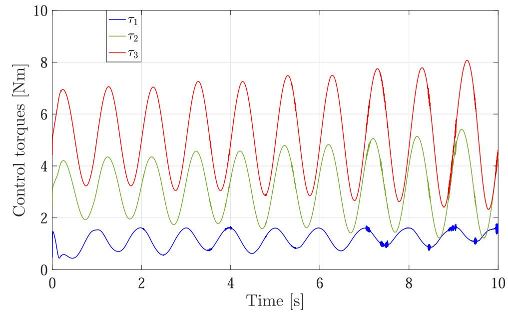

FIGURE 14. The time histories of the control inputs under control design II.

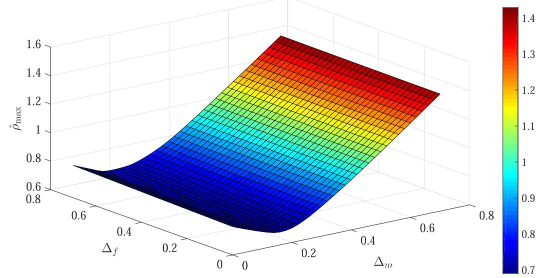

FIGURE 15. Maximum of $\hat{\rho}_{\max}$ with respect to Δ_m and Δ_f under control design II.

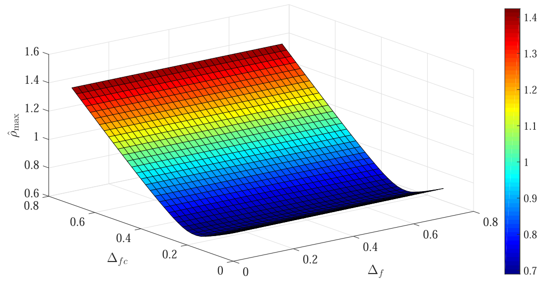

FIGURE 16. Maximum of $\hat{\rho}_{\max}$ with respect to Δ_f and Δ_{fc} under control design II.

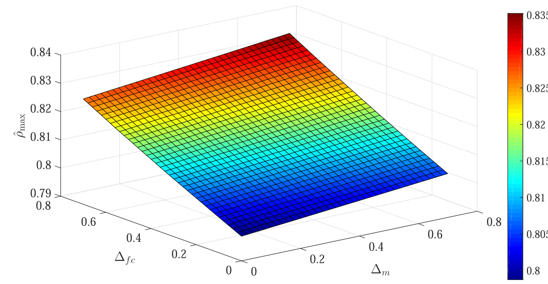

FIGURE 17. Maximum of $\hat{\rho}_{\max}$ with respect to Δ_m and Δ_{fc} under control design II.

It increases quickly from the initial value $\hat{\rho}_0 = 0.02$ to the maximal value $\hat{\rho}_{max} = 0.7$, and decreases with the reduction of the trajectory tracking error. Fig. 8 demonstrates the time histories of the control torques τ_1, τ_2 and τ_3 of driven motors. Let $\hat{\rho}_{\max} = \max_t \|\hat{\rho}\|$. Fig. 9-Fig. 11 demonstrate the effects of the uncertainty bounds Δ_m, Δ_{fc} and Δ_f on $\hat{\rho}_{\max}$.

Second, with the same simulation conditions, the adaptive robust control design II is researched in the following simulations. The simulation results are given in Fig. 12-Fig. 17. Fig. 12 shows the trajectory tracking errors $\|r\|$ and $\|\dot{r}\|$ under control design II. The trajectory tracking error $\|r\|$ quickly enters to a small zone around 0 in less than 0.2 seconds. The trajectory tracking error $\|\dot{r}\|$ is uniform bounded for all $t > 0$ and uniform ultimate bounded for $t \leq 2$s. Fig. 13 is the time history of the adaptive parameter $\hat{\rho}$. As the existence of the leakage term, $\hat{\rho}$ shows tendency to ascend before 2s, then descends to almost 0.5. Fig. 14 shows the time histories of the control torques τ_1, τ_2 and τ_3 of driven motors. Fig. 15-Fig. 17 demonstrate the effects of the uncertainty bounds Δ_m, Δ_{fc} and Δ_f on $\hat{\rho}_{\max}$.

Third, for comparison of the two control designs, the accumulative control torques S (that is the area enclosed by $\|\tau(t)\|$

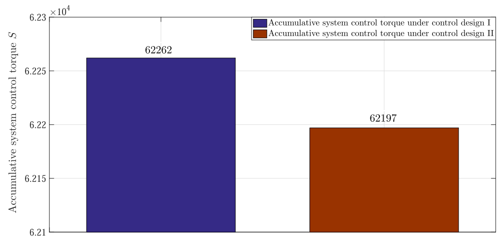

FIGURE 18. The comparison of the accumulative system control torques under two control designs.

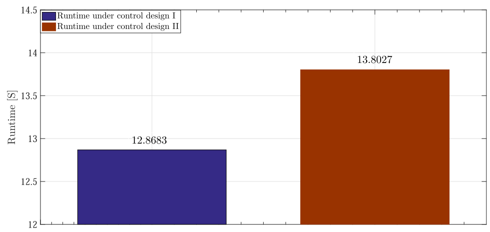

FIGURE 19. The comparison of the runtime under two control designs.

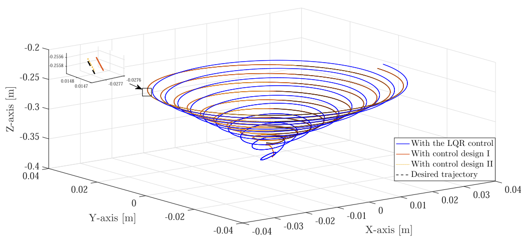

FIGURE 20. The comparison of the end-effector trajectories under different controls for path type I.

and t) is described as:

$$S = \int_0^{T_t} \|\tau(t)\| \, dt, \tag{68}$$

where T_t is the simulation time. In Fig. 18, the accumulative control torques S under the first robust controller design is 62262, on the other hand S under the second robust controller design has a smaller value 62197. Meanwhile, the actual runtimes of the two control designs are calculated in Fig. 19. The runtime of the first robust controller design is 12.8683s and the runtime of the second robust controller design is 13.8027s. Those simulation results indicate that the choice of the first robust controller design or the second robust controller design are decided by the priority of the control cost or the computation speed.

Fourth, for comparison, we adopt a LQR (Linear Quadratic Regulator) controller to carry out a series of simulations. To validate the generality of the proposed control designs, one more desired trajectory (path type II) is chosen

$$\begin{bmatrix} x^d(t) \\ y^d(t) \\ z^d(t) \end{bmatrix} = \begin{bmatrix} 0.1\sin(\pi t) \\ 0.1\cos(\pi t) \\ -0.4 + 0.02t/\pi \end{bmatrix}. \tag{69}$$

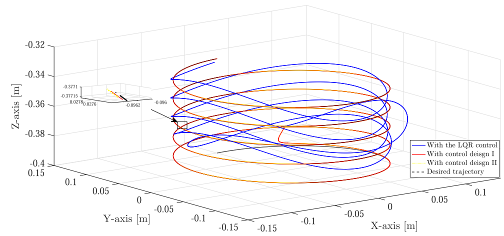

FIGURE 21. The comparison of the end-effector trajectories under different controls for path type II.

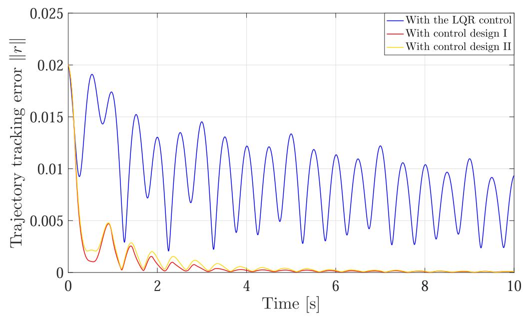

FIGURE 22. The comparison of the trajectory tracking errors $\|r\|$ under different controls for path type I.

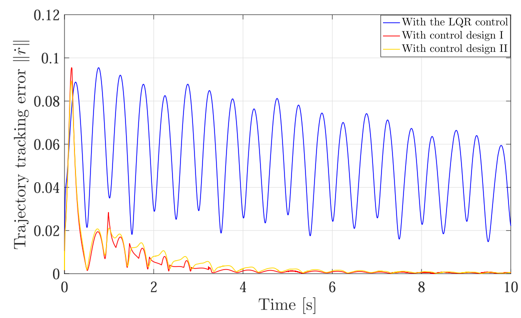

FIGURE 23. The comparison of the trajectory tracking errors $\|\dot{r}\|$ under different controls for path type I.

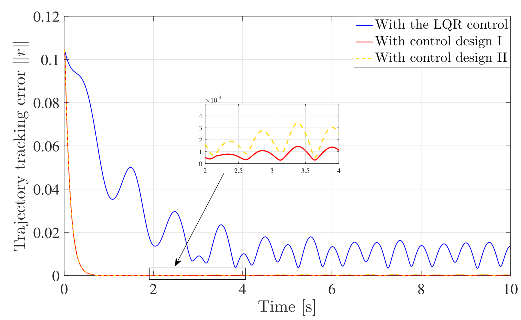

FIGURE 24. The comparison of the trajectory tracking errors $\|r\|$ under different controls for path type II.

Fig. 20-21 demonstrate the end-effector trajectories under the different controls for the two type paths. Comparing with LQR control, the trajectories of the proposed controls are closest to the desired trajectory paths. In Fig. 22-25, the trajectory tracking errors $\|r\|$ and $\|\dot{r}\|$ with LQR control are

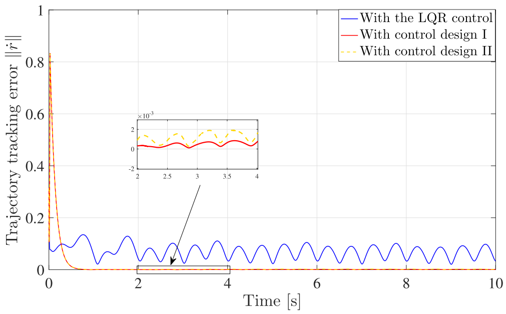

FIGURE 25. The comparison of the trajectory tracking errors $\|\dot{r}\|$ under different controls for path type I.

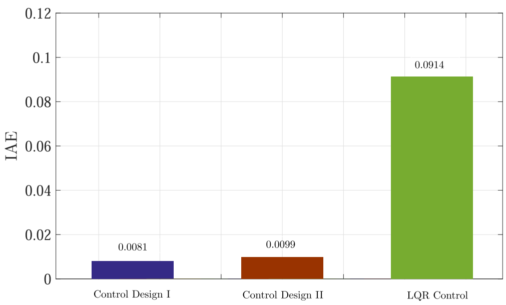

FIGURE 26. The comparison of the integral absolute errors under different controls for path type I.

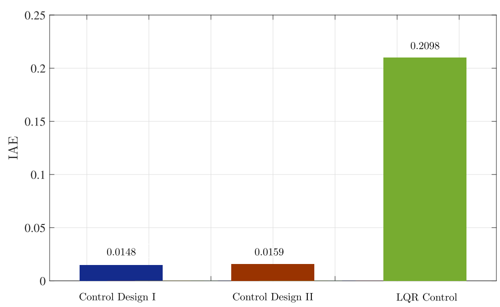

FIGURE 27. The comparison of the integral absolute errors under different controls for path type II.

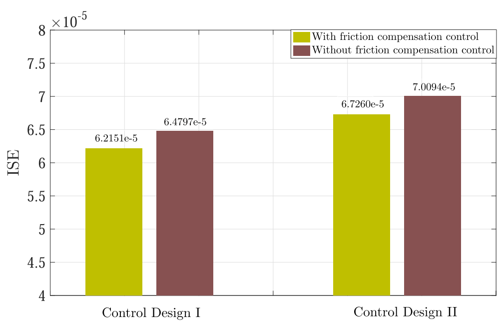

FIGURE 28. The comparison of the integral square errors under different controls for path type I.

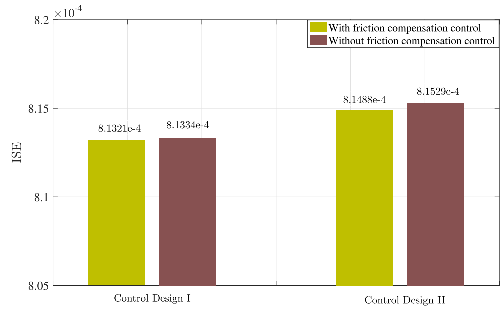

FIGURE 29. The comparison of the integral square errors under different controls for path type II.

bounded but not convergent for both types of paths, no matter how long one waits. While, the errors $\|r\|$ and $\|\dot{r}\|$ with the proposed control design I and design II increase at first and then approximately close to 0 after 2s for path type I, and quickly settle to a very small zone around 0 in less than 0.25 s for path type II. The IAE (integral absolute errors) indices of different controls for two types paths are illustrated by Fig. 26-27. From the results in Fig. 20-27, we conclude that the proposed two robust control designs have far superior performance with respect to LQR control.

Finally, in order to observe the influence of the joints friction on the Delta robot, we implement the simulations without the friction compensation control for the two types of paths. In Fig. 28-29, for both types of paths, the ISE (integral square errors) indices of the proposed control designs without friction compensation control are higher than the controls with the friction compensation control. Hence, the influence of the joints friction should be considered in the Delta robot control design (especially in some sophisticated applications).

VI. CONCLUSION

Based on the online estimation approach, we have proposed a class of novel robust controls for the Delta parallel robot with nonlinearity and uncertainty. To improve the dynamic performance of the Delta parallel robot under the high speed and heavy load condition, we formulate the precise and explicit motion equation of the robot with joints friction. By the constructed motion equation, a nominal control portion containing an active friction compensation is derived via the inverse dynamics. The uncertainty of the Delta parallel robot in the paper includes the unknown dynamic parameters of robot, the vibration of the robot arms, the external disturbances of the end-effector and the time-varying normal forces of the joints friction (caused by the imperfect knowledge of the friction model). Unlike the traditional robust controls (focusing on the probabilistic distribution or the bound of the uncertainty), we design an alternative method to tackle with the uncertainty. An online estimation mechanism, consisting the exponential leakage term and dead-zone, is proposed to search the real-time information of the uncertainty. This estimation method only needs the uncertainty is bounded (which is practical for the robot in applications). It may relieve the engineers from the plentiful investigations of the uncertainty. With the estimated bounds information, two robust controls are designed for the Delta parallel robot with the initial condition deviation, joints friction and uncertainty. Those controls can provide two priorities for the Delta parallel robot between the control efficiency and the control cost (high order design).

REFERENCES

[1] G. Gao, M. Ye, and M. Zhang, "Synchronous robust sliding mode control of a parallel robot for automobile electro-coating conveying," *IEEE Access*, vol. 7, pp. 85838–85847, 2019.

[2] S. Qian, B. Zi, D. Wang, and Y. Li, "Development of modular cable-driven parallel robotic systems," *IEEE Access*, vol. 7, pp. 5541–5553, 2019.

[3] J. E. Correa, J. Toombs, N. Toombs, and P. M. Ferreira, "Laminated micro-machine: Design and fabrication of a flexure-based Delta robot," *J. Manuf. Processes*, vol. 24, pp. 370–375, Oct. 2016.

[4] X.-J. Liu, J. I. Jeong, and J. Kim, "A three translational DoFs parallel cube-manipulator," *Robotica*, vol. 21, no. 6, pp. 645–653, Dec. 2003.

[5] K. C. Olds, "Global indices for kinematic and force transmission performance in parallel robots," *IEEE Trans. Robot.*, vol. 31, no. 2, pp. 494–500, Apr. 2015.

[6] G. Yedukondalu, A. Srinath, and J. S. Kumar, "Mechanical chest compression with a medical parallel manipulator for cardiopulmonary resuscitation," *Int. J. Med. Robot. Comput. Assist. Surgery*, vol. 11, no. 4, pp. 448–457, Oct. 2014.

[7] G. Borchert, M. Battistelli, G. Runge, and A. Raatz, "Analysis of the mass distribution of a functionally extended Delta robot," *Robot. Comput.-Integr. Manuf.*, vol. 31, pp. 111–120, Feb. 2015.

[8] R. Kelaiaia, "Improving the pose accuracy of the Delta robot in machining operations," *Int. J. Adv. Manuf. Technol.*, vol. 91, nos. 5–8, pp. 2205–2215, Jul. 2017.

[9] E. Rodriguez, C. Riaño, A. Alvares, and R. Bonnard, "Design and dimensional synthesis of a linear Delta robot with single legs for additive manufacturing," *J. Brazilian Soc. Mech. Sci. Eng.*, vol. 41, no. 11, p. 536, Nov. 2019.

[10] K. He, Z. Yang, Y. Bai, J. Long, and C. Li, "Intelligent fault diagnosis of Delta 3D printers using attitude sensors based on support vector machines," *Sensors*, vol. 18, no. 4, p. 1298, Apr. 2018.

[11] D. Shang, Y. Li, Y. Liu, and S. Cui, "Research on the motion error analysis and compensation strategy of the Delta robot," *Mathematics*, vol. 7, no. 5, p. 411, May 2019.

[12] L. Rey and R. Clavel, "The Delta parallel robot," in *Advanced Manufacturing*, C. R. Boër, L. Molinari-Tosatti, and K. S. Smith, Eds. London, U.K.: Springer, 1999, pp. 401–417.

[13] T. Su, L. Cheng, Y. Wang, X. Liang, J. Zheng, and H. Zhang, "Time-optimal trajectory planning for delta robot based on quintic pythagorean-hodograph curves," *IEEE Access*, vol. 6, pp. 28530–28539, 2018.

[14] L. A. Castaneda, A. Luviano-Juarez, and I. Chairez, "Robust trajectory tracking of a delta robot through adaptive active disturbance rejection control," *IEEE Trans. Control Syst. Technol.*, vol. 23, no. 4, pp. 1387–1398, Jul. 2015.

[15] J. Fabian, C. Monterrey, and R. Canahuire, "Trajectory tracking control of a 3 DOF delta robot: A PD and LQR comparison," in *Proc. IEEE 23rd Int. Congr. Electron., Electr. Eng. Comput. (INTERCON)*, Piura, Peru, Aug. 2016, pp. 1–5.

[16] M. Rachedi, M. Bouri, and B. Hemici, "Design of an H_∞ controller for the Delta robot: Experimental results," *Adv. Robot.*, vol. 29, no. 18, pp. 1–17, Jul. 2015.

[17] O. Linda and M. Manic, "Uncertainty-robust design of interval type-2 fuzzy logic controller for delta parallel robot," *IEEE Trans. Ind. Informat.*, vol. 7, no. 4, pp. 661–670, Nov. 2011.

[18] G. Leitmann, "On one approach to the control of uncertain systems," *J. Dyn. Syst., Meas., Control*, vol. 115, no. 2B, pp. 373–380, Jun. 1993.

[19] Z. K. Xiong, G. Leitmann, and F. Garofalo, "Robustness of uncertain dynamical dystems with delay in the absence of matching assumptions stochastic games and related topics," in *Theory and Decision Library*, T. E. S. Raghavan, T. S. Ferguson, T. Parthasarathy, and O. J. Vrieze, Eds. Dordrecht, The Netherlands: Springer, 1991, pp. 191–200.

[20] M. Corless, "Control of uncertain nonlinear systems," *J. Dyn. Sys., Meas., Control*, vol. 115, no. 2B, pp. 362–372, Jun. 1993.

[21] Y. H. Chen and G. Leitmann, "Robustness of uncertain systems in the absence of matching assumptions," *Int. J. Control*, vol. 45, no. 5, pp. 1527–1542, Jun. 2010.

[22] A. Codourey, "Dynamic modelling and mass matrix evaluation of the DELTA parallel robot for axes decoupling control," in *Proc. IEEE/RSJ Int. Conf. Intell. Robots Syst. (IROS)*, Osaka, Japan, Aug. 2002, pp. 1211–1218.

[23] J. Hui, M. Pan, R. Zhao, L. Luo, and L. Wu, "The closed-form motion equation of redundant actuation parallel robot with joint friction: An application of the Udwadia–Kalaba approach," *Nonlinear Dyn.*, vol. 93, no. 2, pp. 689–703, Mar. 2018.

[24] H. Olsson, K. J. Astrom, C. D. Wit, and M. Gäfvert, "Friction models and friction compensation," *Eur. J. Control*, vol. 4, no. 3, pp. 5517–5522, Jan. 1998.

[25] Y. H. Chen, G. Leitmann, and J. S. Chen, "Robust control for rigid serial manipulators: A general setting," in *Proc. Amer. Control Conf. (ACC)*, Philadelphia, PA, USA, Jun. 1998, pp. 912–916.

[26] Y.-H. Chen and X. Zhang, "Adaptive robust approximate constraint-following control for mechanical systems," *J. Franklin Inst.*, vol. 347, no. 1, pp. 69–86, Feb. 2010.

RUIYING ZHAO (Member, IEEE) received the Ph.D. degree, in 2015. She visited The George W. Woodruff School of Mechanical Engineering, Georgia Institute of Technology, Atlanta, as a Visiting Ph.D. Student, from September 2012 to September 2014. She is currently a Postdoctoral Research Fellow with Chang'an University, China. Her research interests include multibody system dynamics, robust control of mechanical systems, fuzzy dynamical systems, robot intelligent control, and energy-saving control for construction machinery.

LINLIN WU (Student Member, IEEE) received the M.S. degree in mechanical engineering from Chang'an University, China, in 2018, where she is currently pursuing the Ph.D. degree in mechanical engineering. Her research interests include fuzzy dynamical systems, modelling, and robust control of robot.

YE-HWA CHEN received the Ph.D. degree from the University of California at Berkeley, Berkeley, in 1985. He is currently a Professor with The George W. Woodruff School of Mechanical Engineering, Georgia Institute of Technology. His research interests include fuzzy dynamical systems, fuzzy reasoning, and modeling and control of mechanical systems. He received the IEEE Transactions on Fuzzy Systems Outstanding Paper Award from the IEEE Neural Networks Council, in 2001. He has been serving as a Regional Editor and/or an Associate Editor for six journals.